Hu *et al. Chin. J. Mech. Eng.* (2019) 32:46
https://doi.org/10.1186/s10033-019-0356-4

Chinese Journal of Mechanical Engineering

ORIGINAL ARTICLE

Open Access

A New Method of Wind Turbine Bearing Fault Diagnosis Based on Multi-Masking Empirical Mode Decomposition and Fuzzy C-Means Clustering

Yongtao Hu[1,2], Shuqing Zhang[1*], Anqi Jiang[1], Liguo Zhang[1], Wanlu Jiang[1] and Junfeng Li[1]

Abstract

Based on Multi-Masking Empirical Mode Decomposition (MMEMD) and fuzzy c-means (FCM) clustering, a new method of wind turbine bearing fault diagnosis FCM-MMEMD is proposed, which can determine the fault accurately and timely. First, FCM clustering is employed to classify the data into different clusters, which helps to estimate whether there is a fault and how many fault types there are. If fault signals exist, the fault vibration signals are then demodulated and decomposed into different frequency bands by MMEMD in order to be analyzed further. In order to overcome the mode mixing defect of empirical mode decomposition (EMD), a novel method called MMEMD is proposed. It is an improvement to masking empirical mode decomposition (MEMD). By adding multi-masking signals to the signals to be decomposed in different levels, it can restrain low-frequency components from mixing in high-frequency components effectively in the sifting process and then suppress the mode mixing. It has the advantages of easy implementation and strong ability of suppressing modal mixing. The fault type is determined by Hilbert envelope finally. The results of simulation signal decomposition showed the high performance of MMEMD. Experiments of bearing fault diagnosis in wind turbine bearing fault diagnosis proved the validity and high accuracy of the new method.

Keywords: Wind turbine bearing faults diagnosis, Multi-masking empirical mode decomposition (MMEMD), Fuzzy c-mean (FCM) clustering

1 Introduction

Wind energy is one of the fast growing renewable energy resources, and is going to have remarkable share in the energy market [1]. However, as the reason of long term running in atrocious conditions such as bad weather, variable speeds, alternating and heavy loads, wind turbine inevitably generates various faults [2], which include blades fault, bearing fault, gearbox fault, etc. [3–5]. Bearings are essential components of wind turbine, but the faults are often failed to be alarmed promptly by monitoring systems, resulting in serious damages. Therefore, methods of bearing fault diagnosis timely and accurately are extremely valuable.

Fault feature analysis is the premise of fault diagnosis. The common fault analysis methods include domain analysis, frequency domain analysis and time frequency domain analysis [6]. Time domain analysis is the earliest method used in the mechanical fault diagnosis. The commonly used time-domain indicators include maximum, minimum, mean, mean square root and kurtosis value [7]. Frequency domain analysis such as spectrum and envelope analysis is the most involved method in the mechanical fault diagnosis [8]. However, analysis only relying on time domain or frequency domain cannot meet the needs of the current mechanical fault diagnosis, time-frequency analysis has become a hot research topic [9]. In the past years, time-frequency analysis focused on

*Correspondence: zhshq-yd@163.com
[1] Institute of Electric Engineering, Yanshan University, Qinhuangdao 066004, China
Full list of author information is available at the end of the article

short time Fourier transform (STFT), Wavelet transform (WT), and Wigner-Ville distribution (WVD) [10]. However, it is difficult to obtain high resolution by STFT and WT, and is limited in non-stationary signal analysis [11]. WVD is easy suffered from inevitable cross-term interferences, not suitable for many real applications [12]. EMD is a method of signal processing suitable to nonlinear, non-stationary signal, which can decompose the bearing vibration signal into a series of intrinsic mode functions (IMF) adaptively [13]. Each IMF is an approximate single frequency signal and different IMFs contain a large number of intrinsic features of different frequency bands. Combined with Hilbert transform, bearing fault characteristic frequency can be identified by enveloped normalized amplitude-frequency spectrum and fault type can be determined [14].

However, EMD has the disadvantages of mode mixing [15], and bearing vibration signal contains a large number of different frequency components and easily lead to mode mixing, which affect the accuracy of decomposition seriously. In order to solve the problem, the domestic and foreign experts have done a lot of research and proposed a variety of methods, of which the most famous is ensemble empirical mode decomposition (EEMD) [16] proposed by Wu et al. By adding white noise of finite amplitude to the original signal, EEMD changes the local extremum, making the signal continuous in scale and avoiding fitting error caused by the uneven distribution of the extreme in the cubic spline interpolation, and then mode mixing is restrained.

EEMD can suppress mode mixing, but the white noise added in original signal is difficult to be controlled [17]. Furthermore, multiple decompositions are needed to counteract the effect of noise, result in increasing computational complexity seriously [18]. Masking empirical mode decomposition (MEMD) could overcome the shortcomings of EEMD [19]. However, it adds only one masking signal to the original signal and decomposes the signal by EMD. It does not has the theoretical basis and the determination of masking signal is complex.

This paper proposes an improved method to MEMD, named MMEMD, which can restrain low-frequency component from mixing in high-frequency component effectively in the sifting process, and then suppress the mode mixing by adding multi-masking signals to the signals to be decomposed in different levels. Compared with MEMD, MMEMD can restrain mode mixing better and the masking signal is easy to determine.

In fact, the vibration signals of wind turbine bearing (whether in fault or not) are collected by state monitoring system every day. However, it is a development process for the bearing from normal to fault, and the vibration dataset is large, it is difficult to discover whether fault is failed to be found and what is the fault type. So it is necessary to classify the datasets to confirm whether there is a fault and how many fault types there are. If fault signals exist, the rapid and accurate method is required for further analysis to determine the fault type.

Commonly, fault classification can be realized by conventional time-domain features, such as mean, mean square root. Kurtosis value as input features of Fuzzy c-means (FCM). FCM clustering is an unsupervised learning algorithm, which partition data into a certain number of groups according to certain rules and requirements but does not need a priori knowledge [20]. Owing to the simple, raped, accurate advantages of FCM clustering, it is widely used in mechanical fault diagnosis [21].

In the light of the problem above, a new method named FCM-MMEMD is proposed in this paper. FCM is for classifying the dataset to confirm whether abnormal signals exist. If there are abnormal signals, the improved method MMDMD proposed in this paper is performed to decompose the abnormal signals into different frequency band, and Hilbert envelope is used finally to confirm the fault type. The results of simulation, experiments and application show that the method has the advantages of rapid and accurate diagnosis.

2 Multi-Masking Empirical Mode Decomposition

MMEMD is an improved method of MEMD, both of them are based on EMD. In order to explain the performance and the advantages of MMEMD method, the principle of EMD and MEMD, MMEMD are given first.

2.1 IMF and EMD

Signals are composed of a series of IMF with orthogonality and completeness [22]. Each IMF represents a different vibration, whose instantaneous frequency contains the local characteristics of the signal, and the original signal can be recovered by reconstructing all IMFs [23].

The essence of EMD decomposition is to obtain the IMFs by means of sifting, whose goal is to subtract away the large-scale features of the signal repeatedly until only the fine-scale features remain [24]. For a signal $x(t)$, according the IMF definition, the EMD decomposition can use the envelopes defined by the local maxima and minima. Once the extrema are identified, the upper envelope is obtained by connecting all the local maxima via a cubic spline line. Repeating the procedure for the local minima can obtain the lower envelope. The upper and lower envelopes cover all the data among them and their mean value is designated as $m_1(t)$. Then the first sifting is employed to get the first order mode function of first sifting, $h_1(t)$, as follows [25]:

$$h_1(t) = x(t) - m_1(t). \tag{1}$$

Ideally, $h_1(t)$ satisfies the IMF requirements. However any small knee point in the process of sifting may become a new extremum, which also contains the scale feature and may be omitted in the process of obtaining the upper and lower envelopes. So it does not meet the requirements in fact, and repetition of sifting is needed. The upper and lower envelopes of $h_1(t)$ is constructed and their mean is designated as $m_{12}(t)$. Then the second sifting is employed to get the first order mode function of second sifting, $h_{12}(t)$, as follows:

$$h_{12}(t) = h_1(t) - m_{12}(t). \tag{2}$$

Repeating the above sifting process until the first order mode function of the kth sifting, $h_{1k}(t)$, satisfies the two conditions of IMF:

$$h_{1k}(t) = h_{1(k-1)}(t) - m_{1k}(t). \tag{3}$$

As a result, $h_{1k}(t)$ is the first order IMF of $x(t)$ and designated as $c_1(t)$:

$$c_1(t) = h_{1k}(t). \tag{4}$$

The first order residual component can be obtained by subtracting $c_1(t)$ from $x(t)$ as follows:

$$r_1(t) = x(t) - c_1(t). \tag{5}$$

Since $r_1(t)$ still contains information and should be treated as a new signal and repeat the same sifting process until the residual component becomes a monotonic function from which no more IMFs can be extracted. As a result, the signal $x(t)$ is decomposed into a series of IMFs and a residual component (RES) as follows:

$$x(t) = \sum_{i=1}^{n} c_i(t) + r_n(t). \tag{6}$$

2.2 MEMD Algorithm

Although EMD can decomposes the signal into a series of IMFs. There are mode mixing in the IMFs. MEMD is proposed to overcome the disadvantage of mode mixing. The basic idea is to insert a masking signal in to the original signal to prevent the lower frequency component from being into the IMFs. The algorithm of MEMD can be described as follows.

(1) The original signal $x(t)$ is decomposed by EMD and the first IMF is obtained. The IMF contains the highest frequency component.
(2) The Hilbert transform is performed on the first IMF and the instantaneous frequency is obtained. The frequency of the masking signal is calculated as follows:

$$f_k = \frac{\sum_{i=1}^{n} a(i) f_{ins}^2(i)}{f_{sam} \sum_{i=1}^{n} a(i) f_{ins}(i)}, \tag{7}$$

where f_{sam} is the sample rate, n is the number of sample point, $a(i)$ and $f_{ins}(i)$ is the amplitude and instantaneous frequency of the ith sample point.

(3) Construct the masking signal $s(t)$:

$$s(t) = a_k \sin(2\pi f_k), \tag{8}$$

where $a_k = 1.6$ obtained by the rule of thumb.

(4) Insert the $s(t)$ into $x(t)$ as follows:

$$x_{+m}(t) = x(t) + s(t), \tag{9}$$

$$x_{-m}(t) = x(t) - s(t). \tag{10}$$

(5) Perform EMD on $x_{+m}(t)$ and $x_{-m}(t)$. Take the average of IMFs obtained by $x_{+m}(t)$ and $x_{-m}(t)$ as the final IMFs.

From the algorithm we can see that it performs 3 times EMD on the signal and the essence of MEMD is EMD in fact. Even more the frequency of masking signal is depend on the Hilbert transform and the amplitude is depend on experience. So, the performance of decomposition cannot be guaranteed.

2.3 Principle of MMEMD

To yield a better decomposition result, MMEMD is proposed in this paper. MMEMD changes the accuracy of extreme sampling by adding masking signals of different frequency to the signals to be decomposed in different decomposition levels, which can prevent lower frequency components effectively from being included in high frequency components in the process of sifting, and achieve the suppression of mode mixing as a result. The mathematical principle of MMEMD is as follows.

Take the first level decomposition as an example. The masking signal is constructed according to the frequency and amplitude of original signal:

$$s_m(t) = a_m \sin(2\pi f_m t), \tag{11}$$

where a_m is the amplitude and f_m is the frequency of the masking signal, both of them are not less than original signal. $x_+(t)$ is obtained by adding $s_m(t)$ to the original signal $x(t)$ as follows:

$$x_+(t) = x(t) + s_m(t). \tag{12}$$

According to the Shannon's sampling theorem [26], a signal can be perfectly recovered when its frequency is not greater than half of the sampling frequency. So $x(t)$ can be divided into two parts, $x_l(t)$ whose frequency is less than or equal to $f_m/2$ and $x_h(t)$ whose frequency is greater than $f_m/2$. Eq. (8) can be re-expressed:

$$x_+(t) = x_l(t) + x_h(t) + s_m(t). \tag{13}$$

Suppose that the first maximum of $x_+(t)$ lies at t_1, the sampling point of upper envelope of $x_+(t)$ can be expressed as $e_{up}(t)$:

$$e_{up}(t) = \sum_{k=-\infty}^{\infty} \left[x\left(\frac{k}{f_m} + t_1\right) + a_m \sin(2\pi f_m t_1) \right] \times \operatorname{cosc}[f_m(t - t_1) - k], \tag{14}$$

where $\operatorname{cosc}(t) = \cos(\pi t)/(\pi t)$,$x_l(t)$ does not lose information after extreme sampling but aliasing is unavoidable. Therefore, Eq. (14) can be re-expressed as follows:

$$e_{up}(t) = x_l(t) + x_{up}(t) + a_m \sin(2\pi f_m t_1), \tag{15}$$

$$x_{up}(t) = \sum_{k=-\infty}^{\infty} \left[x_h\left(\frac{k}{f_m} + t_1\right) \right] \operatorname{cosc}[f_m(t - t_1) - k]. \tag{16}$$

Similarly, if the first minimum of $x_+(t)$ locates at t_2, the lower envelope can be written as:

$$e_{dn}(t) = x_l(t) + x_{dn}(t) + a_m \sin(2\pi f_m t_2), \tag{17}$$

$$x_{dn}(t) = \sum_{k=-\infty}^{\infty} \left[x_h\left(\frac{k}{f_m} + t_2\right) \right] \operatorname{cosc}[f_m(t - t_2) - k], \tag{18}$$

where $x_{up}(t)$ and $x_{dn}(t)$ are the high frequency mixing components. The median envelope can be obtained according to Eqs. (15)–(18):

$$e_{mid}(t) = \frac{e_{up}(t)+e_{dn}(t)}{2} = x_l(t) + x_{ud}(t) + \tfrac{1}{2}[a_m \sin(2\pi f_m t_1) + a_m \sin(2\pi f_m t_2)], \tag{19}$$

$$x_{ud}(t) = \frac{1}{2}[x_{up}(t) + x_{dn}(t)]. \tag{20}$$

It is obvious that the masking signal is only a constant in median envelope. Suppose Fourier transform sampling frequency is f_s, $x_{ud}(t)$ can be represented in frequency domain as follows:

$$X_{ud}(j\Omega) = \sum_{i=0}^{D-1} x_h\left(j\frac{\omega - 2\pi i}{D}\right) \times \sin\left[\frac{(D_{dn} - D_{up})\pi i}{D}\right] e^{-j\frac{D_{dn}+D_{up}}{D}\pi i}, \tag{21}$$

where $D = [f_s/f_m]$, $D_{up} = [f_s t_1]$, $D_{dn} = [f_s t_2]$, $\omega = D\Omega/f_s$, the symbol $[\cdot]$ indicates integer part, t_1 and t_2 has the following relationship:

$$t_2 - t_1 = \frac{1}{2f_m}. \tag{22}$$

Ignoring the error generated by the integer operation, Eqs. (23) and (24) can be get:

$$\frac{(D_{dn} - D_{up})}{D} = \frac{1}{2}, \tag{23}$$

$$\frac{(D_{dn} + D_{up})}{D} = (t_2 + t_1)f_m. \tag{24}$$

Therefore, $X_{ud}(j\Omega)$ can be rewritten as follows:

$$X_{ud}(j\Omega) = \sum_{i=0}^{D-1} x_h\left(j\frac{\omega - 2\pi i}{D}\right) \sin(\frac{1}{2}\pi i) e^{-ijf_m\pi i(t_1+t_2)}. \tag{25}$$

Because $\sin(\frac{1}{2}\pi i) = 0$ when i is even and $e^{-ijf_m\pi i(t_1+t_2)} \approx 0$ when i is odd, there is $X_{ud}(j\Omega) \approx 0$. Thus, high frequency mixing components is effectively suppressed and $e_{mid}(t)$ can be re-expressed as follows:

$$e_{mid}(t) = x_l(t) + C, \tag{26}$$

where $C = \frac{1}{2}[a_m \sin(2\pi f_m t_1) + a_m \sin(2\pi f_m t_2)]$, is a constant. According to the EMD method, $c_{1+}(t)$ is obtained by many times sifting of $x_+(t)$:

$$c_{1+}(t) = x_h(t) + s_m(t) - C. \tag{27}$$

$c_{1+}(t)$ is the first IMF of $x_+(t)$, in which low frequency component in original signal is completely eliminated and only high frequency components remained.

Similarly, $x_-(t)$ is obtained by subtracting $s_m(t)$ from the original signal as follows:

$$x_-(t) = x(t) - s_m(t). \tag{28}$$

And the first IMF of $x_-(t)$, $c_{1-}(t)$, is obtained by many times sifting of $x_-(t)$:

$$c_{1-}(t) = x_h(t) - s_m(t) - C. \tag{29}$$

Take the mean of $c_{1+}(t)$ and $c_{1-}(t)$, the first IMF of $x(t)$ is obtained as follows:

$$c_1(t) = x_h(t) - C. \tag{30}$$

As discussed above, the effect of masking signal is to suppress the low-frequency components sneak into high-frequency components. And high frequency components are extracted at each decomposition. It means that the frequency is just required to be between the highest frequency and the sub highest frequency. And the amplitude should be the maximum amplitude of the signal to be decomposed. Both of them are easily determined by examining the peaks of the DFT spectrum.

2.4 MMEMD Algorithm

According to the MMEMD principle, MMEMD decomposition algorithm is as follows.

(1) The DFT spectrum of the original signal $x(t)$ is analyzed, and the decomposition level j and the approximate frequency of each frequency band are determined.
(2) Let $i = 1, x_i(t) = x(t)$.
(3) According to the step (1), the frequency of the adjacent two frequency bands f_{i1} and f_{i2} are determined. The average values are taken as the frequency of the masking signal. The amplitude of the higher frequency component is taken as the amplitude a_{im}. The masking signal, $s_{im}(t)$, is obtained as follows:

$$s_{im}(t) = a_{im}\sin(2\pi f_{im}t). \tag{31}$$

(4) Construct $x_{i+}(t)$ and $x_{i-}(t)$ according to Eqs. (12) and (28).
(5) Obtain $c_{i+}(t)$ and $c_{i-}(t)$ by means of sifting use cubic spline interpolation method. Take average of them and get the $c_i(t)$, which is IMFi.
(6) Subtract $c_i(t)$ from $x_i(t)$ to obtain the $r(t)$, and let

$$r(t) = x_i(t) - c_i(t). \tag{32}$$

(7) Let $x_i(t) = r(t)$ and $i = i + 1$, repeat above steps from (3) until $i = j$ and the j IMFs are obtained.

3 FCM-MMEMD Method

FCM clustering is one of the most commonly discussed and used fuzzy clustering algorithm [27].

Let $X = \{x_1, x_2, \ldots, x_n\}$ donates the fault features, which can be partitioned into c clusters. n represents the mount of the features. Suppose that the cluster center is $v_i (i = 1, 2, \ldots, c)$ and the samples membership function belongs to the cluster i is $u_{ik} (i = 1, 2, \ldots, c, k = 1, 2, \ldots, n)$. Then the objection function of FCM can be defined [28]:

$$J_m(U, v) = \sum_{i=1}^{c}\sum_{k=1}^{n} u_{ik}^m d_{ik}^2, \tag{33}$$

where $d_{ik}^2 = \|x_k - v_i\|^2$, $U = \{u_{ik}\}$, $v = (v_1, v_2, \cdots, v_c)$, $m > 1$ is a constant. And u_{ik} satisfies the following requirements [29]:

$$\sum_{i=1}^{c} u_{ik} = 1, \ \forall k = 1, 2, \ldots, n, \tag{34}$$

$$0 < \sum_{k=1}^{n} u_{ik} < n, \ \forall i = 1, 2, \ldots, c. \tag{35}$$

According to the Lagrange multiplier optimization method, when the object function reaches its minimum, the requirements are:

$$u_{ik} = \sum_{j=1}^{c} d_{jk}^{\frac{2}{m-1}} \Big/ d_{ik}^{\frac{2}{m-1}}, \tag{36}$$

$$v_i = \sum_{k=1}^{n} u_{ik}^m x_k \Big/ \sum_{k=1}^{n} u_{ik}^m. \tag{37}$$

The commonly used clustering performance index is the partition coefficient (PC), the larger the value is, the better the clustering result is [30].

$$PC = \frac{1}{n}\sum_{i=1}^{c}\sum_{k=1}^{n} u_{ik}^2. \tag{38}$$

For the simple principle of FCM clustering, it is applied in bearing fault diagnosis in this paper. Figure 1 is the flowchart of FCM-MMEMD and the process can be detailed as follows.

(1) Sample N points from the bearing signal x. FCM is to confirm whether there are abnormal signals. We calculate mean square root and kurtosis value as the fault features according to Eqs. (39) and (40):

$$X_{\text{rms}} = \sqrt{\sum_{i=1}^{N} x_i^2 \Big/ N}, \tag{39}$$

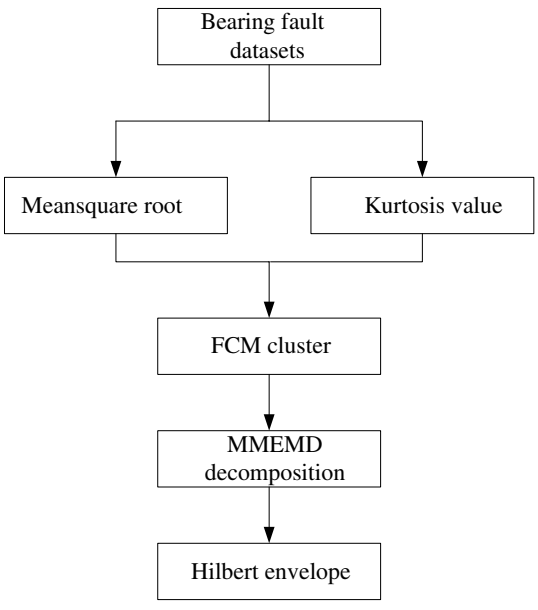

Figure 1 Flowchart of FCM and MMEMD

$$K_v = \sum_{i=1}^{N} x_i^4 \Big/ (N \cdot X_{\text{rms}}^4). \tag{40}$$

(2) Classify the datasets into n categories by FCM clustering. $n = \{1, 2, 3, 4, \ldots\}$ is determined according to the partition coefficient (PC), the bigger of PC, the better of cluster result.
(3) Take one sample from each category and decompose it by MMEMD, different frequency bands (IMFs) are obtained.
(4) Analyze the high frequency component by Hilbert envelope to determine the fault types.

4 Simulation Experiment and Application

In order to improve the high performance of MMEMD and the feasibility of FCM-MMEMD method, simulation signal decomposition, bearing fault diagnosis experiment and wind turbine bearing fault diagnosis application are conducted.

4.1 Decomposition of Simulation Signal by MMEMD

Consider a multi-component signal $x(t)$:

$$x(t) = x_1(t) + x_2(t) + x_3(t), \tag{41}$$

where $x_1(t) = \sin(100\pi t)$, $x_2(t) = 1.5\sin(200\pi t)$ and $x_3(t) = \sin(300\pi t)$, the sample frequency $f = 4000$ Hz and sample time $t = 0.256$ s, so 1024 points are obtained.

First, $x(t)$ was decomposed by EMD, 5 IMFs and a RES were obtained as Figure 2. Pearson correlation coefficients between $x(t)$ and IMFs were calculated as in Table 1. So the most relevant IMFs are IMF1, IMF2 and IMF3. Ideally, IMF1 should be $x_3(t)$, but it contains 3 frequency components, namely 150 Hz, 100 Hz and 50 Hz, because of the effect of mode mixing. And IMF2 should be $x_2(t)$, but the amplitude is significantly reduced.

As discussed above, EMD has the shortcoming of mode mixing, which seriously affects the decomposition results.

Secondly, $x(t)$ was decomposed by EEMD as a comparison. The white noise amplitude was determined as 0.1 and average number was 50 by repeated experiments. Figure 3 is the EEMD decomposing result, which show only IMF1-IMF3 for convenience. From Figure 3 It can be seen that the IMF1 contains 2 frequency components and the amplitude of IMF2 is reduced a little. So EEMD can restrain the mode mixing but cannot avoid mode mixing completely.

Thirdly, $x(t)$ was decomposed by MEMD. According to the method of Ref. [9], the frequency and amplitude

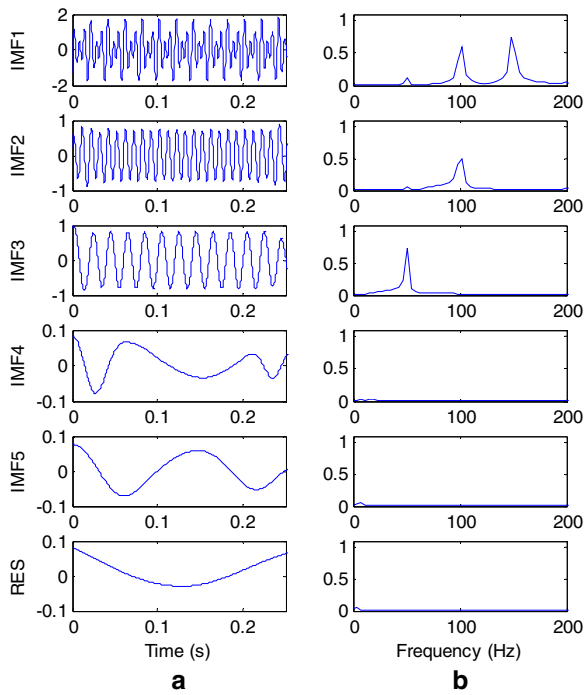

Figure 2 $x(t)$ decomposed by EMD: (**a**) waveform; (**b**) amplitude-frequency characteristic

of the masking signal are obtained as $f_m = 252$, $a_m = 1.6$. The result is shown in Figure 4. It shows that the IMF2 contains 3 components, but the amplitude of the main frequency component is larger than the mixing mode. The result is better than EEMD.

Finally, $x(t)$ was decomposed by MMEMD. DFT spectrum of $x(t)$ is analyzed as Figure 5. From Figure 5, the amplitudes of masking signals are $a_m = 1.5$ and the frequencies are $f_{1m} = 125$, $f_{2m} = 75$. The decomposition result is shown in Figure 6. It shows that IMF1 contains component of 150 Hz and 100 Hz, but the amplitude of 100 Hz is very small. And the amplitude of IMF2 was not reduced, so there is no mode mixing.

Table 2 is the evaluating indicator of the four decomposition methods. RMSE is the root mean square error between the IMFs and the corresponding frequency components of the original signal. TC is the time consuming of the decomposition methods. It shows that the MMEMD has the smallest RMSE, indicating that the IMF obtained by MMEMD can represent the different frequency components of the original signal well. Moreover, it can be seen that the EMD has the shortest time consuming, and the EEMD has the longest time consuming, which is about 80 times as much as EMD. The time consuming of MMEMD is little longer than EMD but it can be accepted compared to avoiding the mode mixing.

Table 1 Pearson correlation coefficients

IMF1	IMF2	IMF3	IMF4	IMF5	RES
0.8647	0.7445	0.5004	0.0444	0.0323	0.0456

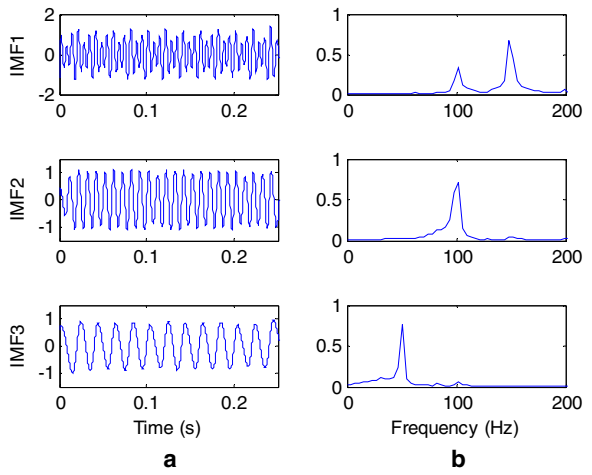

Figure 3 $x(t)$ decomposed by EEMD: (**a**) waveform, (**b**) amplitude-frequency

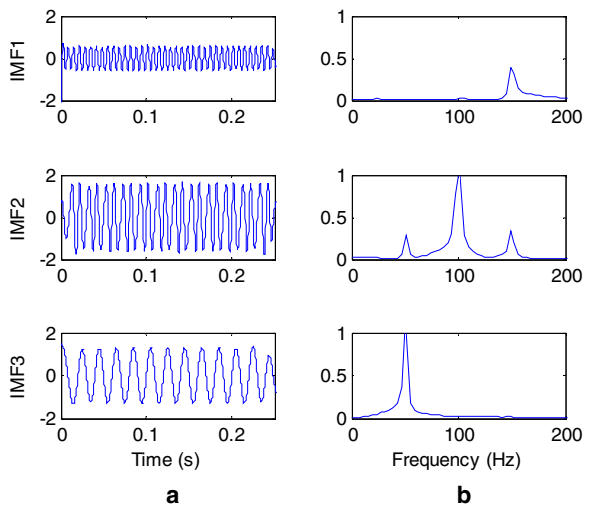

Figure 4 $x(t)$ decomposed by MEMD: (**a**) waveform, (**b**) amplitude-frequency

4.2 Bearing Fault Diagnosis Experiment

Bearing fault diagnosis experiment was carried out in order to verify the validity and superiority of FCM-MMEMD method. Bearing vibration data was collected from the bearing fault diagnosis experiment rig [31]. It consists of a 1.47 kW motor, a torque transducer/encoder, a dynamometer, and control electronics. The type of bearing is SFK6205. Single point faults with diameters of 0.007 inches in ball, inner raceway and outer raceway were introduced to the test bearings by electro-discharge. The motor speed was 1750 r/min, load was 1.47 kW and sampling frequency was 12 kHz. The fault characteristic frequency of the ball fault, inner raceway fault and outer raceway fault are respectively 57.5 Hz, 157.9 Hz and 104.6 Hz. For each kind of signal (normal was included), 10 samples were collected and the total samples is 40. X_{rms} and K_{ν} were calculated and normalized listing in Table 3. FCM cluster was employed to classify these samples and the cluster result is shown in

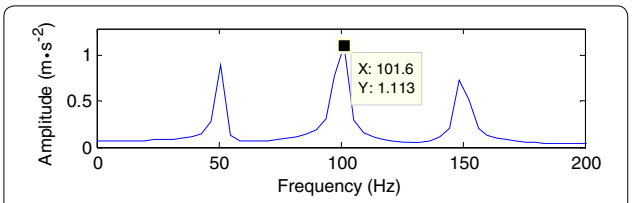

Figure 5 DFT spectrum of $x(t)$

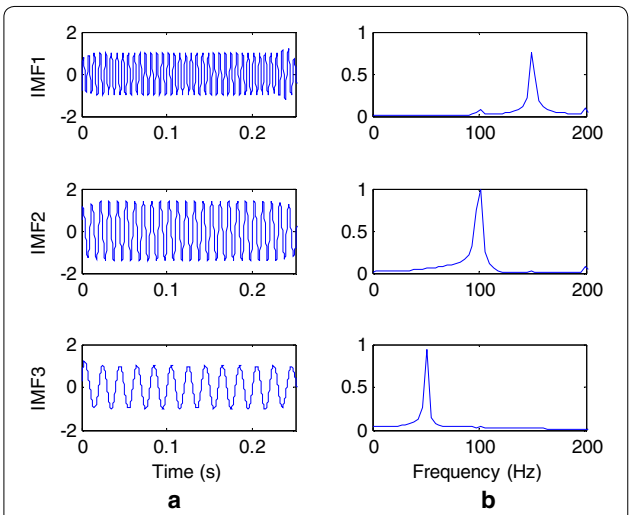

Figure 6 $x(t)$ decomposed by MMEMD: (**a**) waveform, (**b**) amplitude-frequency

Table 2 Evaluating indicator of 3 decomposition method

Method	Evaluating indicator			
	RMSE1	RMSE2	RMSE3	TC (s)
EMD	0.5564	0.5610	0.1731	0.0308
EEMD	0.3286	0.4196	0.1903	23.4909
MEMD	0.3580	0.3921	0.2587	0.1831
MMEMD	0.1880	0.2138	0.1152	0.4375

Table 3 X_{rms} **and** K_v **of different samples**

Sample	X_{rms}	K_v
1	0.0203	0.0356
2	0.4453	0.5360
3	0.1389	0.0292
4	0.9335	0.8405
⋮	⋮	⋮

Figure 7. It is clearly that the samples are classified into 4 categories. That means there are 4 bearing states. But what are the states need more analysis.

A sample was decomposed by MMEMD in order to verify the high accuracy of MMEMD to bearing fault vibration signal decomposition. Figure 8 is the waveform and amplitude-frequency characteristic of three high frequency components obtained by MMEMD. It can be seen that the shock characteristic is more obvious than the MEMD shown as Figure 9. From Figure 9, it can be seen that the frequency components of 2000 Hz to 3000 Hz are mixed in the IMF1, denoting that there is mode mixing when the bearing signal is decomposed by MEMD. So MMEMD can restrain the mode mixing better than MEMD.

In conclusion, MMEMD can decompose the bearing signal into different frequency bands effectively, and is beneficial to fault diagnosis accurately.

Take a sample from each categories and decompose them by MMEMD. Hilbert envelope was employed to the highest frequency component shown in Figure 10. It is easily to find the fault characteristic frequency and its fold frequency when the bearings are in failure.

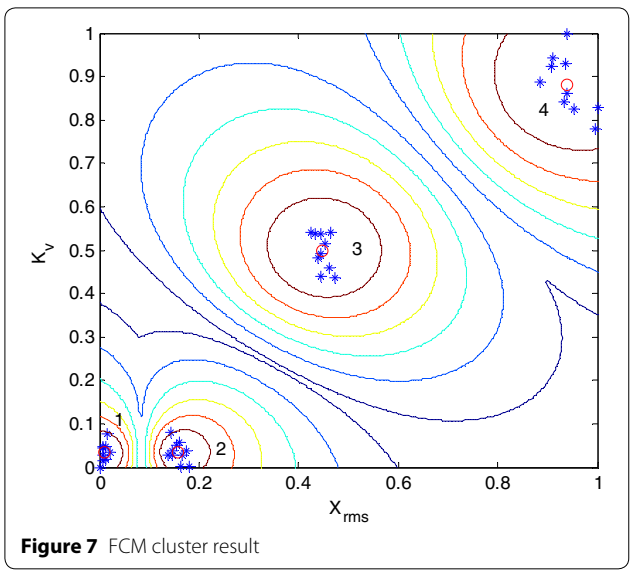

Figure 7 FCM cluster result

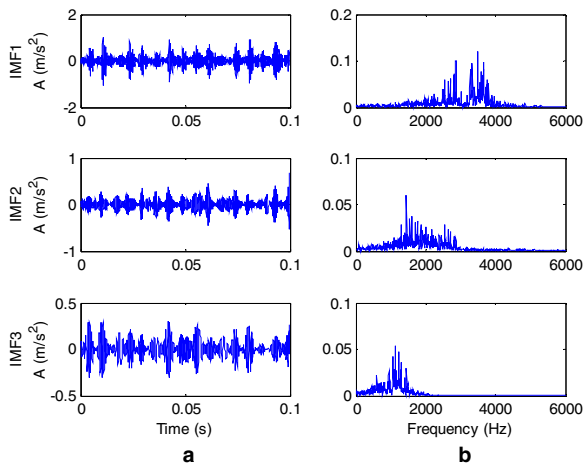

Figure 8 Bearing signal MMEMD decomposition result: (**a**) waveform, (**b**) amplitude-frequency characteristic

According to the fault characteristic frequency, bearings from top to bottom are normal, ball fault, inner raceway fault and outer raceway fault. Let us look back Figure 7. According to Figure 7, if the signals can be clustered in different clusters, it can be sure that there were abnormal signals. Further analysis of the samples of each cluster by MMEMD and Hilbert envelope, the fault type can be determined.

4.3 Application of the Method

The data was collected from a 2 MW wind turbine with a condition monitoring system. For the reason of alarm failure, the high speed bearing is damaged seriously. The vibration signals of high speed bearing were sampled at 10 min intervals every day. The sample rate was 97656 Hz and sample time was 6 s. The unit was Gs, where 1*g* is the earth standard gravitational acceleration. Figure 11 is the acceleration sensor fixed to the high speed bearing. The high speed shaft is driven by a 20 teeth gear, the rated speed is 1800 r/min. According to the rated speed, the fault characteristic frequency of the ball fault, inner raceway fault and outer raceway fault are respectively 86.1 Hz, 284.3 Hz and 201.8 Hz.

For the reason of condition of wind turbine bearing, the speed is changing along the time shown as Figure 12. It is clearly that the high speed bearing signal is non-stationary.

Figure 13 is the waveform and the amplitude-frequency characteristic of the high speed bearing at one day. The high speed bearing is gradually damaged but the condition monitoring system had not given an alarm seasonable until it damaged seriously.

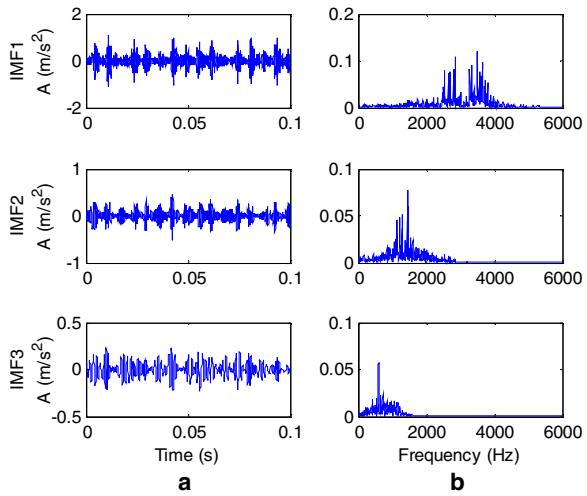

Figure 9 Bearing signal MEMD decomposition result: (**a**) waveform, (**b**) amplitude-frequency characteristic

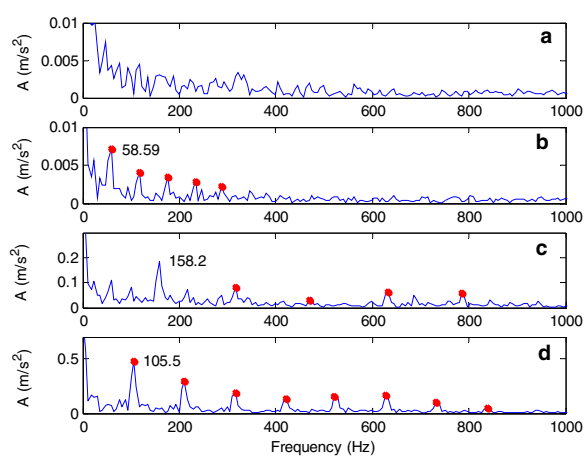

Figure 10 Hilbert envelope of 4 categories: (**a**) normal, (**b**) ball fault, (**c**) inner raceway fault, (**d**) outer raceway fault

Figure 11 Acceleration sensor fixed to high speed bearing

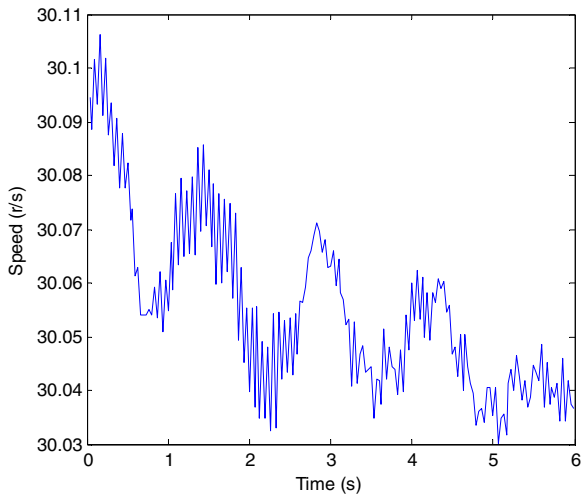

Figure 12 Speed changing along the time

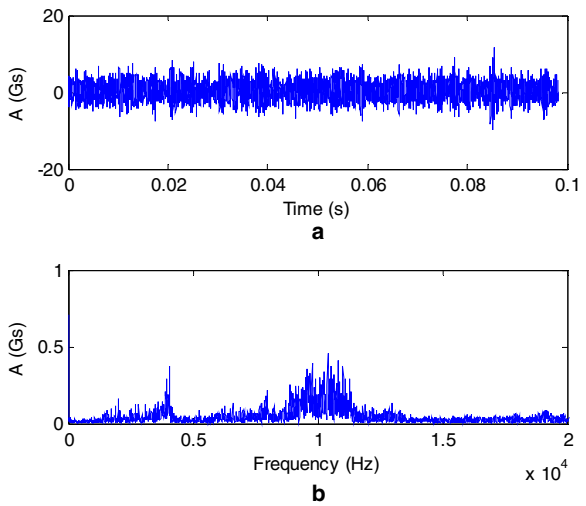

Figure 13 High speed bearing signal: (**a**) waveform, (**b**) amplitude-frequency characteristic

FCM-MMEMD method was implemented for 50 days data. Figure 14 is the FCM cluster result and the data is clustered into 3 classes, namely there are 3 bearing states. Take a sample from each class for further analysis.

Figure 15 is the waveform and IMF1 Hilbert envelope of the three samples. It is clear that sample 1 (day11) is normal for there is neither shock in waveform nor fault characteristic frequency in Hilbert envelope. Sample 2 (day34) are the signals with fault, because fault characteristic frequency of 280.1 Hz (corresponding to inner raceway fault, 284.3 Hz) can be found in Hilbert

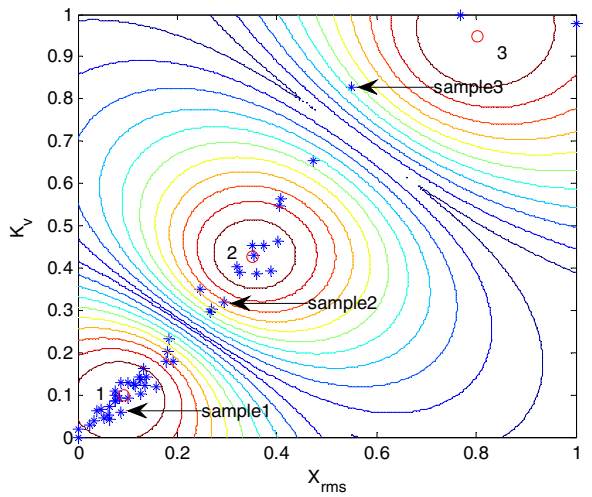

Figure 14 FCM cluster result of high speed bearing

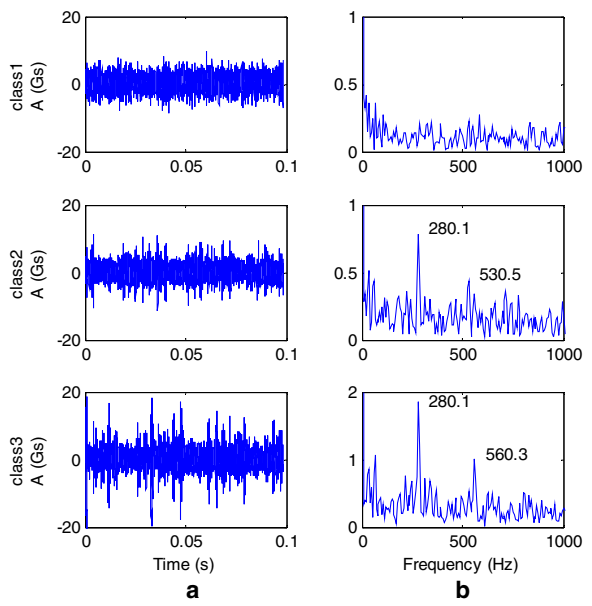

Figure 15 Waveform and IMF1 Hilbert envelope of three classes: (**a**) Waveform, (**b**) Hilbert envelope

envelope. And also there are shocks in waveform. However, the 2 octave frequency is not clear and the shocks are slight, so the fault of simple 2 is a slight damage in inner raceway. For sample 3 (day48), there are both serious shocks in waveform and fault characteristic frequency in Hilbert envelope, and the 2 octave frequency is more obvious than that in sample 2. Therefore sample 3 is in serious damage condition.

According to the above analysis, the bearing was damaged from day34 and became serious later day and

Figure 16 Inner raceway fault bearing

day. However, the condition monitoring system did not alarm until the bearing damaged seriously. Figure 16 is the damaged bearing when it is serviced after 50 days later. It appeared a serious crack and the power quality was seriously declined. But, by the FCM-MMEMD method, when a sample is clustered into class 2 (abnormal signal), it should be focused on. In order to ensure the normal operation of the wind turbine and production of high quality power, the wind turbine should be maintained at day34 to prevent the situation from becoming worse.

As a conclusion, the method can find the mechanical fault accurately and timely, which is important to the maintenance of the equipment.

5 Conclusions

(1) A new bearing fault diagnosis method FCM-MMEMD is presented. The abnormal signals could first be detected by FCM, and be further analyzed by MMEMD and Hilbert envelope to determine the fault type.

(2) MMEMD is an improvement of MEMD, which can restraint the mode mixing better and can be conducted more easily. Simulation to signals decomposition showed that MMEMD could decompose signals into different frequency bands fast and accurately.

(3) Experiments of bearing fault diagnosis and application of wind turbine bearing fault diagnosis proved that the method could diagnosis the bearing fault timely and accurately.

Authors' Contributions

SZ was in charge of the whole trial; YH, AJ and LZ wrote the manuscript; YH, WJ and JL assisted with sampling and laboratory analyses. All authors read and approved the final manuscript.

Author Details
[1] Institute of Electric Engineering, Yanshan University, Qinhuangdao 066004, China. [2] School of Electrical Engineering and Automation, Henan Institute of Technology, Xinxiang 453003, China.

Authors' Information

Yongtao Hu, born in 1987, is currently a lecturer at *Henan Institute of Technology, China*. He received his PhD degree from *Yanshan University, China*, in 2017. His research areas are signal processing and fault diagnosis.

Shuqing Zhang, born in 1966, is currently a professor at *Institute of Electrical Engineering, Yanshan University, China*. She received her PhD in Measuring/Detection Technique and Instrumentation from *Yanshan University, China*, in 2003. Her research areas are the intelligent signal process, measuring instrument and fault diagnosis.

Anqi Jiang, born in 1995, is currently studying for a master's degree at *Institute of Electrical Engineering of Yanshan University, China*. She received her B.S. degree from the *Information Science and Engineering College, Central South University, China,* in 2017. Her research areas include nonlinear adaptive control system and machine learning.

Liguo Zhang, born in 1978, is currently an associate professor at *Yanshan University, China*. He received his B.S. degree from *Beijing Institute of Science and Technology, China*, in 2001, his M.S. degree and Ph.D. degree from *Yanshan University*, *China*, in 2004 and 2010. His research areas include fault diagnosis, machine motion perception and virtual reality technology.

Wanlu Jiang, born in 1964, is currently a professor at *Institute of Mechanical Engineering, Yanshan University, China*. He received his PhD degree in Control Science and Engineering from *Yanshan University, China*, in 2001. His research areas are the intelligent signal process, measuring instrument and fault diagnosis.

Junfeng Li, born in 1994, is currently studying for a master's degree at *Institute of Electrical Engineering of Yanshan University, China*. He received his B.S. degree from *Yanshan University, China*, in 2016. His research areas are signal processing and fault diagnosis.

Competing Interests

The authors declare that they have no competing financial interests.

Funding

Supported by National Key R&D Projects (Grant No. 2018YFB0905500), National Natural Science Foundation of China (Grant No. 51875498), Hebei Provincial Natural Science Foundation of China (Grant Nos. E2018203439, E2018203339, F2016203496), and Key Scientific Research Projects Plan of Henan Higher Education Institutions (Grant No. 19B460001).

Received: 14 January 2019 Accepted: 19 April 2019
Published online: 16 May 2019

References

[1] D Warts, N Oses, R Perez. Assessment of wind energy potential in Chile: A project-based regional wind supply function approach. *Renewable Energy*, 2016, 96: 738–755.
[2] I Attoui, A Omeiri. Modeling, control and fault diagnosis of an isolated wind energy conversion system with a self-excited induction generator subject to electrical faults. *Energy Conversion and Management*, 2014, 82(82): 11–26.
[3] S Raza, H Mokhils, H Arof, et al. Application of signal processing techniques for islanding detection of distributed generation in distribution network: A review. *Energy Conversion and Management*, 2015, 96(88): 613–624.
[4] R P Shao, W T Hu, X A Huan, et al. Multi-damage feature extraction and diagnosis of a gear system based on higher order cumulant and empirical mode decomposition. *Journal of Vibration and Control*, 2013, 21(4): 736–754.
[5] A Humeauaeurtier, P Abraham P, G Mahe G. Analysis of laser speckle contrast images variability using a novel empirical mode decomposition: comparison of results with laser Doppler flowmetry signals variability. *IEEE Transactions on Medical Imaging*, 2015, 34(2): 618–627.
[6] Y Cui, J Shi, Z Wang. System-level operational diagnosability analysis in quasi real-time fault diagnosis: The probabilistic approach. *Journal of Process Control*, 2014, 24(9): 1444–1453.
[7] S Nandi, H A Toliyat, X Li. Condition monitoring and fault diagnosis of electrical motors—A review. *IEEE Transactions on Energy Conversion*, 2005, 20(4): 719–729.
[8] J Wang, Q He, F Kong. Multiscale envelope manifold for enhanced fault diagnosis of rotating machines. *Mechanical Systems and Signal Processing*, 2015, s 52–53(1): 376–392.
[9] Z P Feng, X W Chen, M Liang, et al. Time–frequency demodulation analysis based on iterative generalized demodulation for fault diagnosis of planetary gearbox under nonstationary conditions. *Mechanical Systems and Signal Processing*, 2015, 62–63: 54–74.
[10] M Zeng, Y Yu, J D Zheng, et al. Normalized complex teager energy operator demodulation method and its application to rotor rub-impact fault diagnosis. *Journal of Mechanical Engineering*, 2014, 50(5): 65–73. (in Chinese)
[11] A Tabrizi, L Garibaldi, A Fasana, et al. Influence of stopping criterion for sifting process of empirical mode decomposition (EMD) on roller bearing fault diagnosis. *Lecture Notes in Mechanical Engineering*, 2014: 389–398.
[12] S Guo, Y C Xu, X S Li, et al. Research on roller bearing with fault diagnosis method based on EMD and BP neural network. *Advanced Materials Research*, 2014, 1014(1014): 501–504.
[13] N E Huang, Z Shen, S R Long, et al. The empirical mode decomposition and the Hilbert spectrum for nonlinear and non-stationary time series analysis. *Proceedings Mathematical Physical and Engineering Sciences*, 1998, 454(1971): 903–995.
[14] D J Yu, J S Cheng, Y Yang. Application of Hilbert-Huang transform method to gear fault diagnosis. *Journal of Mechanical Engineering*, 2005, 41(6): 102–107. (in Chinese)
[15] Hu X, Peng S, Hwang W L. EMD revisited: A new understanding of the envelope and resolving the mode-mixing problem in AM-FM signals. *IEEE Transactions on Signal Processing*, 2011, 60(3): 1075–1086.
[16] Z H Wu, N E Huang. Ensemble empirical mode decomposition: A nosis-assited data analysis method. *Advances in Adaptive Data Analysis*, 2011, 1(01): 1–41.
[17] M Zhang, T Jian, X Zhang, et al. Intelligent diagnosis of short hydraulic signal based on improved EEMD and SVM with few low-dimensional training samples. *Chinese Journal of Mechanical Engineering*, 2016, 29(2): 396–405.
[18] L Chen, G S Tang, Y Y Zi, et al. Improved EEMD applied to rotating machinery fault diagnosis. *Applied Mechanics & Materials*, 2012, 128–129: 154–159.
[19] R Deering, J F Kaiser. The use of a masking signal to improve empirical mode decomposition. *IEEE International Conference on Acoustics, Speech, and Signal Processing*, Philadelphia, March 18–23, 2005: 485–488.
[20] T Velmurugan. Performance based analysis between k-Means and Fuzzy C-Means clustering algorithms for connection oriented telecommunication data. *Applied Soft Computing*, 2014, 19(6): 134–146.
[21] W L Jiang, Z W Wang, Y Zhu, et al. Fault recognition method for rolling bearing integrating VMD denoising and FCM clustering. *Journal of Information and Computational Science*, 2015, 12(16): 5967–5975.
[22] M Li, F C Li, B B Jing, et al. Multi-fault diagnosis of rotor system based on differential-based empirical mode decomposition. *Journal of Vibration and Control*, 2015, 21(9): 1821–1837.
[23] Y G Lei, Z J He, Y Y Zi. Application of the EEMD method to rotor fault diagnosis of rotating machinery. *Mechanical Systems and Signal Processing*, 2009, 23(4): 1327–1338.
[24] C Wang, M Gan, C Zhu. Non-negative EMD manifold for feature extraction in machinery fault diagnosis. *Measurement*, 2015, 70(6): 188–202.
[25] Y B Li, M Q Xu, W Yu, et al. An improvement EMD method based on the optimized rational Hermite interpolation approach and its application to gear fault diagnosis. *Measurement*, 2015, 63: 330–345.
[26] A J Jerri. The Shannon sampling theorem—Its various extensions and applications: A tutorial review. *Proceedings of the IEEE*, 1977, 65(11): 1565–1596.
[27] A Biniza, A Abbasi. Fast FCM with spatial neighborhood information for Brain Mr image segmentation. *Journal of Artificial Intelligence and Soft Computing Research*, 2016, 3(1): 15–26.

[28] C L Feng, D Z Zhao, M Huang. Image segmentation using CUDA accelerated non-local means denoising and bias correction embedded fuzzy c-means (BCEFCM). *Signal Processing*, 2016, 122(C): 164–189.
[29] H J Sun, S R Wang, Q S Jiang. FCM-based model selection algorithms for determining the number of clusters. *Pattern Recognition*, 2004, 37(10): 2027–2037.
[30] Y K Dubey, M M Mushrif. FCM clustering algorithms for segmentation of Brain MR images. *Advances in Fuzzy Systems*, 2016, (2016-3-15), 2016, 2016(3): 1–14.
[31] Bearing Data Center. Seeded fault test data. http://csegroups.case.edu/bearingdatacenter/pages/download-data-file. 2013-10-15/2015-04-08.